Nanotube–antibody biosensor arrays for the detection of circulating breast cancer cells

2008 Nanotechnology 19 465101

(http://iopscience.iop.org/0957-4484/19/46/465101)

Nanotechnology **19** (2008) 465101 (11pp) doi:10.1088/0957-4484/19/46/465101

Nanotube–antibody biosensor arrays for the detection of circulating breast cancer cells

Ning Shao[1], **Eric Wickstrom**[2,3] **and Balaji Panchapakesan**[1,4]

[1] Delaware MEMS and Nanotechnology Laboratory, Department of Electrical and Computer Engineering, University of Delaware, Newark, DE 19716, USA
[2] Department of Biochemistry and Molecular Biology, Thomas Jefferson University, Philadelphia, PA 19107, USA
[3] Kimmel Cancer Center, Thomas Jefferson University, Philadelphia, PA 19107, USA
[4] Department of Mechanical Engineering, University of Louisville, 247 Belknap Research Building, Louisville, KY 40292, USA

E-mail: b0panc01@louisville.edu

Received 20 May 2008, in final form 16 August 2008
Published 21 October 2008
Online at stacks.iop.org/Nano/19/465101

Abstract

Recent reports have shown that nanoscale electronic devices can be used to detect a change in electrical properties when receptor proteins bind to their corresponding antibodies functionalized on the surface of the device, in extracts from as few as ten lysed tumor cells. We hypothesized that nanotube–antibody devices could sensitively and specifically detect entire live cancer cells. We report for the first time a single nanotube field effect transistor array, functionalized with IGF1R-specific and Her2-specific antibodies, which exhibits highly sensitive and selective sensing of live, intact MCF7 and BT474 human breast cancer cells in human blood. Those two cell lines both overexpress IGF1R and Her2, at different levels. Single or small bundle of nanotube devices that were functionalized with IGF1R-specific or Her2-specific antibodies showed 60% decreases in conductivity upon interaction with BT474 or MCF7 breast cancer cells in two μl drops of blood. Control experiments with non-specific antibodies or with MCF10A control breast cells produced a less than 5% decrease in electrical conductivity, illustrating the high sensitivity for whole cell binding by these single nanotube–antibody devices. We postulate that the free energy change due to multiple simultaneous cell–antibody binding events exerted stress along the nanotube surface, decreasing its electrical conductivity due to an increase in band gap. Because the free energy change upon cell–antibody binding, the stress exerted on the nanotube, and the change in conductivity are specific to a specific antigen–antibody interaction; these properties might be used as a fingerprint for the molecular sensing of circulating cancer cells. From optical microscopy observations during sensing, it appears that the binding of a single cell to a single nanotube field effect transistor produced the change in electrical conductivity. Thus we report a nanoscale oncometer with single cell sensitivity with a diameter 1000 times smaller than a cancer cell that functions in a drop of fresh blood.

(Some figures in this article are in colour only in the electronic version)

1. Introduction

Identification and quantitation of numerous biological molecules to generate a complex molecular profile is required for diagnosis, monitoring, and prognostic evaluation of complex diseases such as cancer. Despite outstanding progress in the area of cancer biology, significant challenges remain in translating biological knowledge of cancer surface markers into clinically relevant devices that could be used as diagnostic or monitoring tools for cancer management. Developing high-throughput diagnostic cell and tissue analysis for disease detection has remained a challenge, however [1]. Techniques for multiplexed

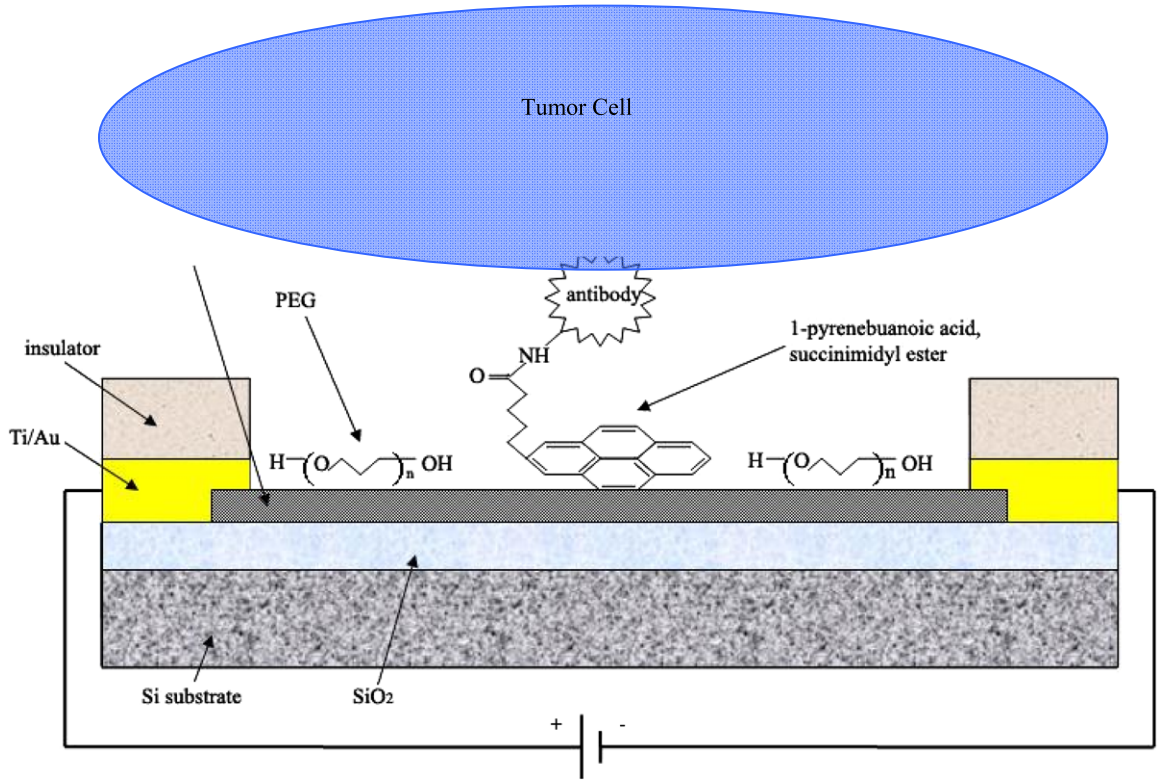

Figure 1. Schematic of the device to illustrate device design, antibody functionalization, and a single 8–12 μm tumor cell binding to the nanotube–antibody (SWCNT-mAb) device. The nanodevice junction is only 1 μm across, bridged by a single 10–20 nm thick SWCNT. These physical parameters preclude the binding of more than one cell at a time. As a result, each SWCNT-mAb junction is an on–off quantum bit.

analysis of extracted proteins for disease monitoring can be divided into four different categories: (1) radioactive and fluorescent reporting of antigen–antibody binding [2–4]; (2) time-of-flight mass spectroscopy [5, 6]; (3) electrophoretic separation and antigen–antibody binding [6]; and (4) detection of changes in surface mechanical and electrical properties due to antigen–antibody binding [7–15]. Although they all have their individual strengths, none of these techniques can directly detect circulating cancer cells that overexpress characteristic surface receptors.

While protein analysis using nanowires [15] presents an attractive approach to monitoring cancer, this technology currently cannot be adopted to detect cancer among populations that are not close to a laboratory or a hospital without significant modification. The same limitations apply to detection of proteins [16] and nucleic acids [17] in physiological fluids and extracts by conductivity changes in carbon nanotube field effect transistor (FET) networks. Similarly, there is not a single technology today that can detect single live cancer cells without extensive instrumentation and highly trained personnel [18, 19].

Combining the knowledge of cancer biology, molecular targeting, and nanotechnology, however, might enable the design of portable or hand-held devices for diagnosis, monitoring, and treatment of cancer appropriate for community or field use. Figure 1 illustrates our model for direct sensing of breast cancer cells by a nanotube–antibody device that interacts with cell surface receptors. The device is designed to have small spacing between the electrodes (1 μm) in order to capture a single live cell (8–12 μm) by specific interaction with their cell surface receptors. Nanotubes that are anchored to the electrodes are functionalized with antibodies that are specific to the IGF1 and Her2 receptors on breast cancer cells. The entire device is isolated using a polymer. Hence, any change in electrical conductivity should arise due to the interaction of the adsorbed antibodies with their targeted receptors on the cell surface upon binding to the nanotube between the electrodes.

Circulating breast cancer cells in the blood are observed more frequently at advanced clinical stages (TNM pStage III and IV) than at early stages (pStage I and II) [20]. Insulin-like growth factor 1 receptor (IGF1R) and human epithelial growth factor receptor 2 (Her2) are frequently overexpressed in breast cancer development and progression [21–24]. Human BT474 breast cancer cells express high levels of *HER2* mRNA, while MCF7 breast cancer cells express much less [25]. Conversely, MCF7 cells overexpress about twice as much IGF1R protein as BT474 cells [26].

Previously we reported receptor-specific detection of MCF7 and BT474 breast cancer cells suspended in physiological buffer with a nanotube–antibody FET [27]. Here we report for the first time the electrical detection of BT474 and MCF7 breast cancer cells added to fresh human donor blood resulting from breast cancer cell binding to single nanotube FETs modified with specific antibodies against IGF1R or Her2. While we use live cells for demonstrating this bioassay, the sensing area is limited to few receptors in cells. Therefore, this technology may potentially enable sensing of small levels of proteins, DNA or even single cells covering the entire spectrum

of molecular sensing to create molecular profiles of single cells over a period of time. It is suggested that the binding of multiple antibodies functionalized on the surface of the nanotubes to multiple sites in the cells, creates a change in free energy and stress across the surface of the nanotube thereby altering its electrical conductivity.

2. Experimental details

The single wall carbon nanotube transistor arrays consisted of two columns of 10 transistors per column. Each junction was monitored independently. One side of the array was used for detecting cells that overexpress IGF1R overexpression and the other side of the array is used to detect cells that overexpress Her2. This allows multiple cell recognition in a single hand-held chip about 1 cm × 1 cm. Such arrays were also used for control experiments. The electrodes in the arrays were patterned using optical lithography, gold metalization and lift-off processes widely used in modern semiconductor industries. Therefore the devices can be fabricated at low cost using batch fabrication techniques. The gap between the electrodes was ∼1 μm and the length of the nanotubes that we used ranged from 1 to 10 μm.

20 mg SWCNT soot, commercially obtained from Nano-Lab (Lot Number FH-P071706), was dissolved in 100 ml methanol and agitated for 24 h in an ultrasonicator (Fisher Scientific, FS60H) at 80 °C to separate the highly entangled SWCNTs to individual or small bundle. The solution was sedimented at 16 100 × g for 30 min and the supernatant, primarily containing individual SWCNTs, was collected while the pellets were discarded. A spray nozzle driven by 65 psi compressed nitrogen with approximately 15 000 sccm volume flow rate was exploited to airbrush 0.5 ml SWCNT solution onto a 1 cm × 1 cm SiO_2 wafer. After the evaporation of methanol, the sample was studied under Jeol JSM-7400F scanning electron microscope to evaluate the partial alignment of the carbon nanotubes.

One μm thick AZ5214 photoresist was applied to the airbrushed SiO_2 wafer and defined by standard photolithography and developing procedures. Excess SWCNTs not fully or partially covered by photoresist were disassociated by ultrasonication in distilled water for ∼10 min (prolonged sonication was avoided to prevent damage to photoresist). Titanium thin film of 10 nm thick was thermally deposited before the 90 nm thick biocompatible gold film to provide better adhesion than just pure gold. The metal contacts were lifted off by the dissolution of photoresist in acetone. The wafer was again ultrasonically agitated to remove SWCNTs not anchored by either metal contact. Devices were then annealed at 400 °C for 5 min under the protection of nitrogen/argon to reduce the contact resistance and further improve the sensitivity of the device. Finally, the devices were covered with SU8 polymer to insulate the surrounding areas of the devices from biomolecules in liquids so as to minimize the noise. The devices were attached to an HP8466 semiconductor parameter analyzer on a Signatone S1160 probe station to detect and record the electrical signals.

Succinimidyl 1-pyrenebutanoate (AnaSpec Inc.) adsorbs onto the sidewalls of SWCNTs through π-stacking and does not dissociate detectably unless oxidized [16]. After adsorption and washing, the succinimide ester crosslinks with exposed amino sidechains of proteins by displacement of N-hydroxysuccinimide. Thus 5 mg of succinimidyl 1-pyrenebutanoate was dissolved in 50 ml methanol, in which the SWCNT airbrushed wafer was incubated for ∼30 min at room temperature with gentle agitation to form a monolayer on the side wall of SWCNTs. After these incubation steps, devices were rinsed three times in DI water to remove any residual reagents.

Non-specific mouse anti-human myeloma immunoglobulin G (IgG) [Catalog Number 411550], anti-IGF1R mouse monoclonal antibody Ab-3 [33255.111, EMD Biosciences] and anti-HER2 monoclonal antibody [Cat. No. OP.39] (Merck Bioscience, Calbiochem Inc.) were dissolved in phosphate-buffered saline (PBS) solution (Mediatech Inc.) at concentrations from 0.5 to 3 μg ml^{-1} were used to incubate the transistors for 3 min at room temperature. To evaluate the binding effect of antibody, samples were studied using Jeol JEM-2000FX transmission electron microscope as shown in figure 5. Poly(ethylene glycol) (PEG) (Acros, average mass 8000 Da), 5 mg, dissolved in 100 ml DI water was applied to each SWCNT-mAb junction to form a PEG monolayer on unoccupied side walls to minimize non-specific biomolecule immobilization during experiments. Adsorption of a pyrenebutanoyl succinimide on side wall of nanotube to crosslink the antibody does not create a covalent bond to the nanotube.

The malignant human breast cancer cell lines MCF7 and BT474, which overexpress different levels of IGF1R and Her2 [21], and non-malignant MCF10A human breast cells were purchased from American Type Culture Collection (ATCC). Cells were incubated with 2 mM glutamine, 5000 U ml^{-1} penicillin, 50 μg ml^{-1} streptomycin and 10% fetal bovine serum in DMEM at 37 °C under 5% CO_2 for 48 h before experiments. MCF7 cells were incubated with additional 7.5 nM 17-β-estradiol. Cells released from culture dishes by EDTA were sedimented at 1000 × g for 5 min. Cell pellets were re-suspended in PBS. 1 μl of cell suspensions containing about 100 000 cells was allowed to flow on the chip to make contact with the nanotube between the electrodes.

Experiments with blood were conducted with fresh human blood volunteered by one of the authors before each experiment. First a single nanotube device that was functionalized with anti-IGF1R mAb was exposed to fresh blood to investigate any potential bio-fouling of devices. For experiments with cells, 1 μl of the cell suspension containing 100 000 cells was mixed with 1 μl of blood and the resulting suspension applied to a single junction on the chip to make contact with the SWCNT-mAb between the electrodes.

3. Results

Figure 2 is an optical image of an SWCNT FET chip array, consisting of 20 pairs of electrodes with a single carbon nanotube between each pair. The nanotubes were anchored between the pairs of electrodes by airbrushing. Figure 3 is an SEM image of the airbrushed SWCNT on a silicon wafer. It is

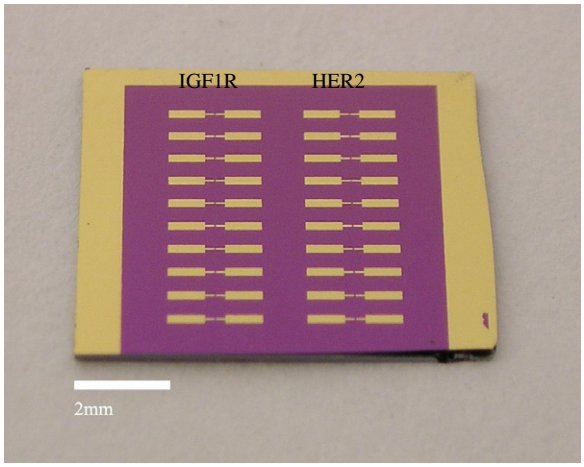

Figure 2. Optical micrograph of a single chip for multicomponent electro-mechanical sensing of IGF1R and Her2 surface receptors in breast cancer cells.

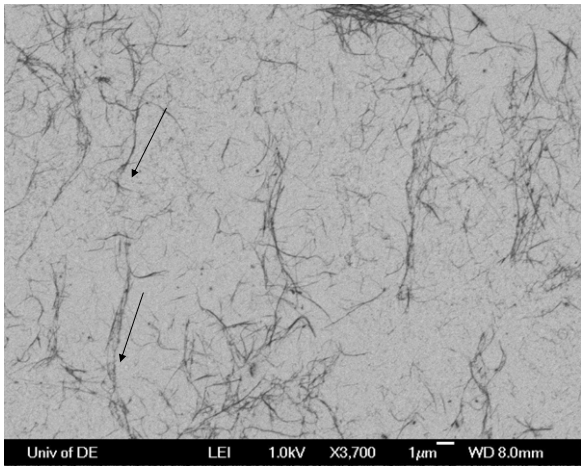

Figure 3. Partial alignment of single wall carbon nanotubes using air brushing. The vertical airflow generated a torque that caused the nanotubes to align.

observed that most of the airbrushed carbon nanotubes were well separated. The simple airbrushing technique provided a certain degree of SWCNT alignment along the direction of air flow, in agreement with existing literature [28, 29]. While airbrushing nanotubes for partial alignment has been reported in the past [28, 29], this study is the first to adapt this technique to semiconductor batch fabrication techniques. The result is faster and lower cost production of single nanotube devices, compared to e-beam lithography.

Electron beam lithography is used widely for top-down manufacturing of nanodevices. However, e-beam lithography is a serial process, slow requiring long exposure times, requires an SEM and vacuum systems for electron beam scanning and expensive. For the purpose of generating a complex molecular profile including a wide variety of biological molecules, the cost of using e-beam lithography-based devices for single bioassay becomes prohibitive. Furthermore, our devices show similar performance and are easy to fabricate, thereby allowing

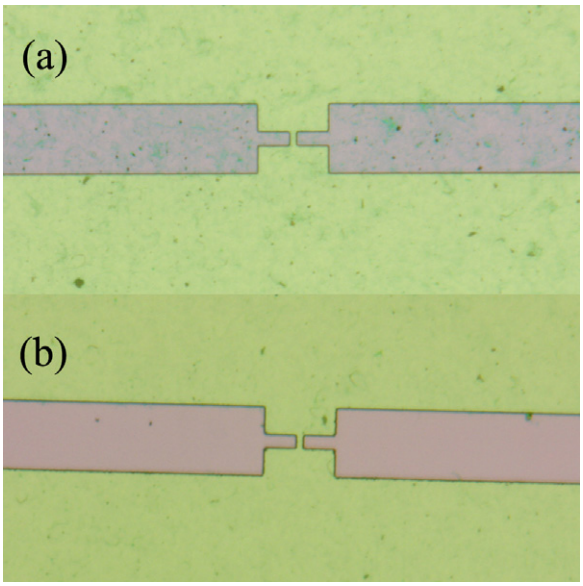

Figure 4. Optical image taken before (a) and after (b) sonication removal of SWCNT. Purple and yellow-greenish areas are bare SiO_2 wafer surface and AZ5214 photoresist respectively. Undesirable SWCNT (light greenish) residing in the purple areas were removed by ultrasonication.

the possibility of large scale production of nanostructure devices for future application in bioassays.

Figure 4 shows the optical image of the airbrushed carbon nanotube device on an oxide wafer after optical lithography. First, photoresist is applied on airbrushed carbon nanotubes and photolithography is performed to define the patterns. After lithography, the nanotubes that are not covered by photoresist are removed by gentle ultrasonic agitation in distilled water for 10 min. Figure 3 shows optical images of the device before and after cleaning by ultrasonic agitation. It is clearly seen that most of the nanotubes around the photoresist are removed completely. Following this procedure, the contact metals were deposited and photoresist lifted off in acetone, thereby leaving SWCNT anchored between the electrodes as seen in the SEM image of figure 5. The inset in figure 5 is the high magnification image of the device showing a single nanotube anchored between the electrodes. The spacing between the electrodes is 1 μm and the nanotube diameter is $\sim$15 nm from the inset in figure 5.

A typical breast cancer cell, in contrast, has a diameter of 8–12 μm [26]. These physical parameters preclude the binding of more than one cancer cell at a time. Thus, one would predict that each SWCNT-mAb junction will function as an on–off quantum bit. Figure 6 presents transmission electron micrograph (TEM) of antibodies functionalized on the surfaces of the carbon nanotube. Our published procedure [26] works well for non-specific, anti-IGF1R, and anti-Her2 antibodies. The TEM images provided direct confirmation that the antibodies aggregate on the surface of the nanotube at many different sites. This has also been confirmed in the past using atomic force microscopy (AFM) and confocal microscopy [26, 30]. Potentially each group of carbon atoms equal to the cross-sectional area of the constant region of a

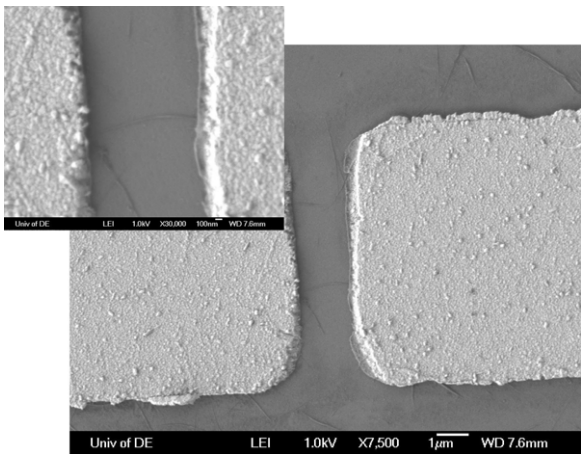

Figure 5. SEM image of a pair of electrodes fabricated by airbrushing and dual sonication techniques. No excessive SWCNTs were observed in the 1 μm wide conduction channel. The inset shows that the electrodes are bridged by SWCNT, 15 nm thick (a small bundle consisting of 10 nanotubes).

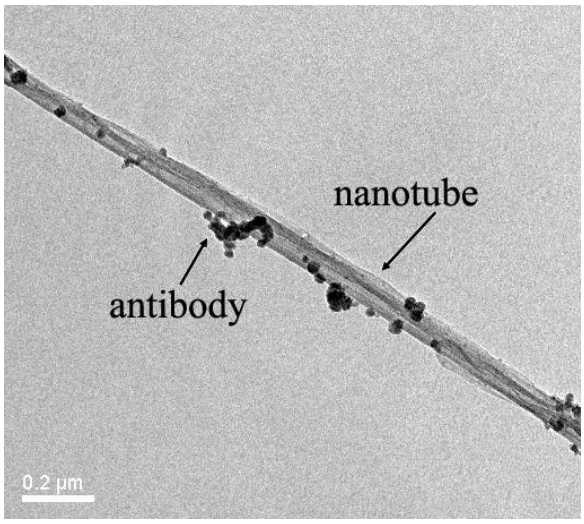

Figure 6. TEM image of the functionalized nanotube with antibodies. Only a single 8–12 μm cancer cell can bind across the 1 μm nanodevice junction.

monoclonal antibody (mAb) constitutes a binding site in the SWCNT that can transport into a living cell. Past AFM studies have shown nanotube–antibody hybrids to be 5–8 nm for a single nanotube functionalized with antibodies [30]. From figure 6, it can be seen that nanotube–antibody hybrids to be ∼100 nm. Subtracting the diameter of the nanotube, ∼15 nm, makes the effective height of the antibodies atop the nanotube ∼85 nm. Therefore it is expected that about 10–12 units of aggregated mAb are bound to SWCNT. Since the devices were rinsed three times in DI water following functionalization, it is expected that all the antibodies are strongly adsorbed to the carbon nanotube.

The transfer characteristics of the devices before antibody functionalization fit the criteria for a p-type SWCNT transistor, showing a strong decrease in source–drain current with

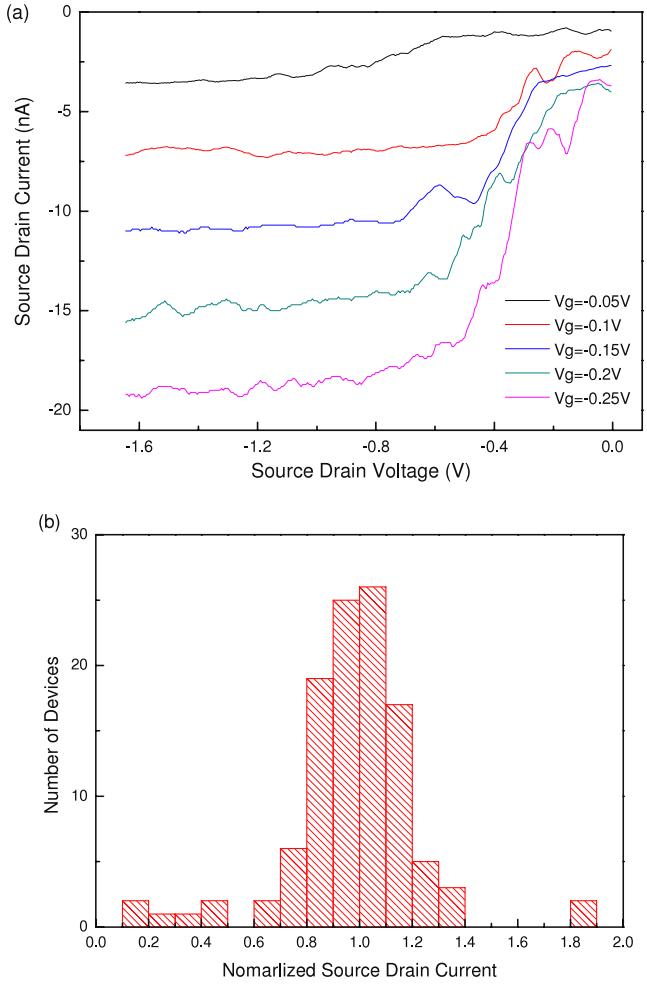

Figure 7. (a) Transfer function of a tested transistor (b) distribution of normalized source–drain currents of devices. The gate and source–drain voltages were set to 0 and 150 mV respectively. Individual source–drain current was divided by the average source–drain current of that chip.

increasing gate voltage as shown in figure 7(a). This also shows that the transport in SWCNT is through holes (positive charge carriers). This is in line with previous reports [31, 32]. The amounts of SWCNTs deposited on each substrate varied, leading to different source–drain currents. However, the transistors' performances on an individual chip were very similar because the density of nanotubes distributed across the relatively small chips was uniform under a single airbrushing run. In order to test this concept, 120 functional transistors on eight different chips showing highly uniform source–drain currents after normalization were plotted in figure 7(b). The distribution of source–drain current at 150 mV source to drain voltage shows a clear Gaussian fit, showing most devices had similar transfer characteristics. Only 80% of the devices acted as p-type FETs while the rest of the devices acted as conductors with metallic characteristics. This demonstrates that the airbrushing technique is statistically acceptable to obtain large numbers of similar devices with similar characteristics. The reason for such comparison with previously reported literature is to establish that the airbrushing technique used to make the

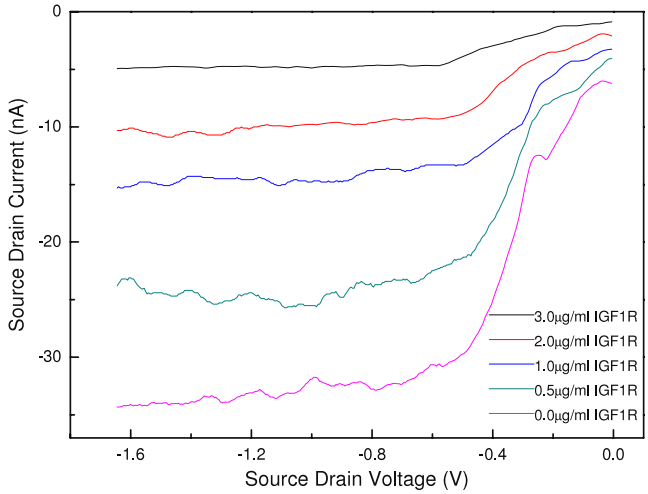

Figure 8. Biomolecular tuning of transfer characteristics for different concentrations of IGF1R antibodies.

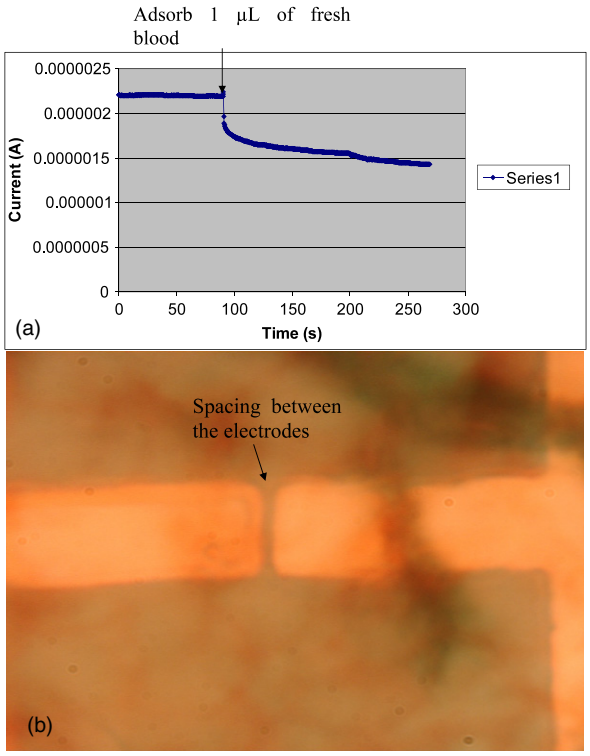

Figure 9. Nanodevice reaction to fresh whole human donor blood. (a) Plot of normalized conductance over time upon dispensing 1.0 μl of blood (arrow) onto the device. (b) Optical micrograph of the device after electrical recording, showing spacing between the electrodes.

devices are quite comparable and the performance acceptable to that of other types of fabrication techniques.

Figure 8 presents the effects of increasing antibody concentration on the nanotube FET. The device behaves like a p-type semiconducting FET due to the depletion of current at all antibody concentrations tested. The abrupt drop indicated that antibodies began adsorbing onto the side wall and SWCNT became more resistive since antibodies tend to suppress current. This shows biomolecular tuning of the transfer characteristics of the transistor. The negatively charged antibodies deplete the current with increasing source to drain voltage. This is similar to initial studies conducted on charge transfer to the nanotube from adsorbed proteins [33]. Even for smaller proteins such as streptavidin, the presence of amine groups donate charge to the nanotube transistor thereby shifting the device characteristics. It was shown that for streptavidin system consisting of 4000 amine groups, each amine group can donate charge of 0.04 electrons to the nanotube thereby lowering the conductivity of the device. It is the presence of these amine groups in the antibodies that lowers the device conductivity.

The mechanism of antibody decreasing the conductance could arise from electrostatic gating effect and Schottky barrier effect in nanotube transistors [34]. However, since our device electrodes were passivated using photo resist as a last step, the undesirable Schottky barrier effect is eliminated. The mechanism of sensing biomolecules is therefore due to electrostatic gating in carbon nanotube transistors. Adsorbates such as antibody donate charge and alter the electrostatic field around the carbon nanotube. There is a strong decrease in conductance of the channel with increasing antibody concentration showing the modulation of transfer characteristics purely due to electrostatic gating. Recent literature has also shown that it is the electrostatic gating that dominates the actual mechanism of sensing biomolecules in nanotube transistors [34].

The size of the nanoscale devices makes them attractive to make hand-held devices that can potentially sense cancer proteins directly from blood. However, it was not clear whether blood cells would foul the device. Therefore, direct adsorption of blood onto the surface of antibody functionalized nanotube was investigated. These devices consisted of network of nanotubes patterned between electrodes figure 9 presents the results of 1 μl of human blood applied to the nanotube–antibody device. Figure 9(a) presents the electrical signal on 1 μl blood adsorption. An optical image of the device after recording of the electrical characteristics was imaged using a video camera mounted to a probe station, shown in figure 9(b). The current in the devices dropped from 22.5 to $\sim$15 μA and stabilized at that level, showing lack of fouling of the device by human blood. The higher current in this device was due to the larger number of nanotubes as against single nanotube devices. Subsequent experiments for detection of cancer cells were conducted in blood. We postulate that the lack of fouling is due to the design of the device, including the PEG coating, and the spacing between the electrodes (1 μm), which is too small for a single cell (8–12 μm) to enter the spacing between the electrodes and foul the device. The change in the device characteristics due to blood adsorption can be explained based on the net surface charge in red blood cells [35]. Mammalian red blood cells have a net surface charge of 7.34×10^2 e.s.u with 15.4×10^{-6} surface electrons per cell. The presence of surface electrons in the blood cells can therefore lower the capacitance of the nanotube device thereby lowering the current. Since the device consisted of large number of nanotubes compared to single nanotube device, it is reasonable to expect larger lowering of current compared to single nanotube device due

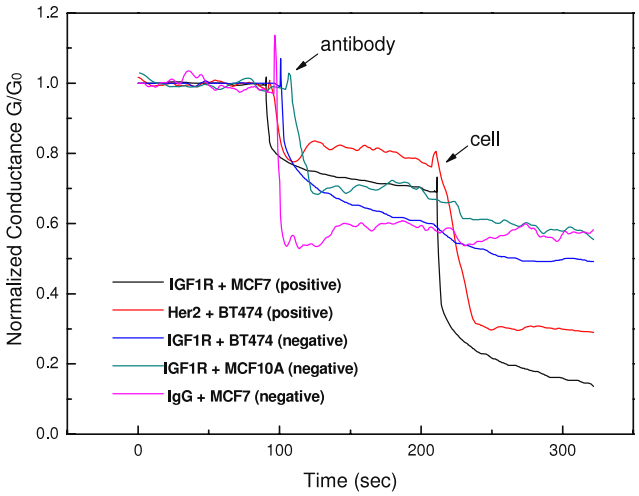

Figure 10. Change in normalized conductance when antibody and cancer cells mixed in blood were applied to the device. Antibodies and cells were dropped at about 100th s and 220th s. Two specific pairs of antibody and cell showed about 60% conductance reduction and three non-specific pair had little impact.

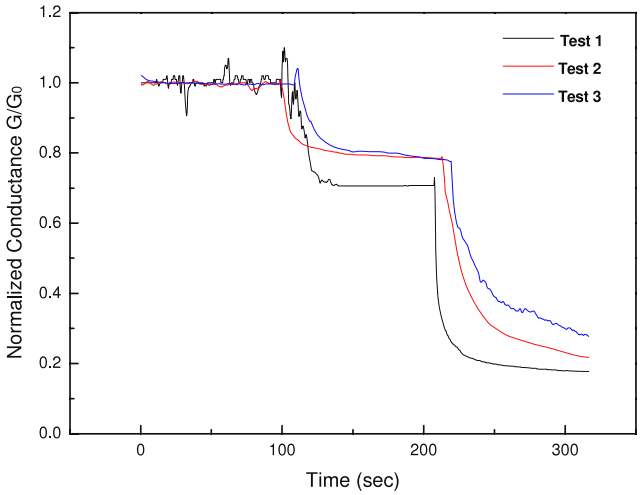

Figure 11. Change in normalized conductance from three different devices that were functionalized with IGF1R and adsorbed with MCF7 breast cancer cells.

to the higher probability of blood cells coming in contact with nanotubes in networked devices than in single nanotube devices.

Figure 10 presents the change in normalized conductance in testing with cancer cells. First the mAb were functionalized onto the surface of the SWCNT and the conductance was recorded from a single junction. After the conductance reached a stable value, cells were applied to the device. One μl of BT474 or MCF7 cancer cells were mixed with 1 μl of fresh human donor blood; 2 μl of the solution, containing ~100 000 breast cancer cells, were applied to the surface of the device using a micropipette. The change in conductance from a single junction was recorded using a semiconductor parameter analyzer with femto-amp accuracy. As one can see from the graphs, there are clear differences. The device that was functionalized with anti-IGF1R antibodies followed by adsorption of MCF7 cells showed 60% reduction in the conductivity, which is the largest. Devices that were functionalized with non-specific antibodies followed by adsorption of MCF7 cells showed less than 10% change in the normalized conductance. This was also true for non-malignant MCF10A cells, which do not overexpress IGF1R [26]. These results indicate clear differences in the change in conductivity between non-specific and specific pairs. It is safe to say two things from these results: (1) the change in conductance is greater for specific pairs compared to non-specific pairs, (2) the change in conductance for all the control cells look similar. Therefore, the change in conductance should originate from the binding of multiple antibodies on the surface of the nanotube to some of the cell surface receptors. One thing is for sure: there is a difference in electrical signal of the device when adsorbed with blood with and with out cancer cells. All these experiments were conducted at least three times to ensure reproducibility.

Figure 11 presents the change in normalized conductance in testing with cancer cells in blood from three different devices to investigate whether the reproducibility of results. All three devices showed similar changes in conductance when functionalized with anti-IGF1R antibodies followed by adsorption of MCF7 cancer cells in blood. The results in figure 11 (which was from a different array) are very similar to the experiment in figure 10. The differences in normalized conductance between different devices were less than 10% showing that there should be biomolecular binding event that cause this change in electrical device characteristics.

When cells mixed with blood were applied to the device, it was difficult to obtain a clear optical image due to subsequent clotting. In order to image cells landing between the device electrodes, we performed preliminary experiments with AsPc1 cancer cells (ATCC) in PBS. Figure 12 presents two images that were captured using a video camera just after applying 1 μl of cancer cells on the device. As one can see from figure 12, while there are many cells on the surrounding area, but only one cell appears to adsorb to the surface between the electrodes, associated with the change in conductivity. In other words, while there may be 100 000 cells in the drop atop the device, it appears that the change in conductivity was due to the binding of only one cell. Also, since all other areas of the SWCNT were completely isolated with insulating PEG coating, the conductivity change for that junction could only occur due to an electron exchange process that occurred between the electrodes that were anchored with an SWCNT-mAb. Once a cell lands between the electrodes, the presence of the electric field between the electrodes from the applied bias also helps to immobilize the cell between the electrodes. Therefore we estimate that the binding of a single cancer cell to adsorbed mAb on the SWCNT device led to the recorded changes in conductivity.

4. Discussion

The binding of antibodies to their corresponding antigens creates a change in free energy that in turn can generate

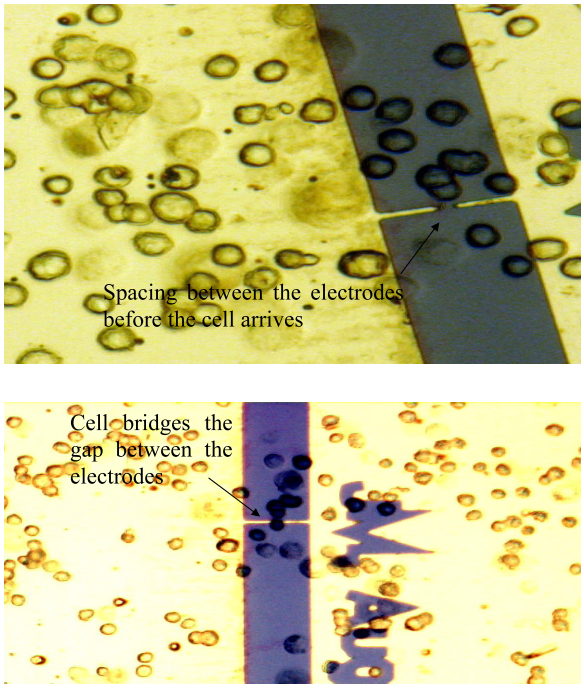

Figure 12. (a) Optical image captured using a video camera of cells arriving at the electrode, (b) cells bridge the gap between the electrode (false color image to illustrate the single cell bridging the electrode). These cells are AsPC1 pancreas cancer cells in PBS.

stress on a surface [36]. This has been used in the past to create bioassays of prostate specific antigens using deflections of a micro-cantilever due to compressive stresses generated as a result of the change in free energy [37]. ΔG^{o} of antigen–antibody interactions fall in the range 11–18 kcal mol^{-1} [38]. We estimated a minimum of 10–12 antigen–antibody interactions between a 10 μm cancer cell contacting a 15 nm $\times$ 1 μm SWCNT-mAb. Thus the minimum estimate for ΔG^{o} of cancer cell-device binding is approximately 10 interactions $\times -15$ kcal mol^{-1} $=$ -150 kcal mol^{-1}.

Our results show that cancer cell binding to cognate antibodies on a nanotube device alters the electron transport properties of the nanotube. Since the nanotubes are not free to deflect and are constrained between electrodes, one is left with the explanation that the nanotubes undergo strain that changes the electron transport properties. This hypothesis is supported by the theory of electron transport in single wall carbon nanotubes that predicted that strain can have a large effect on the band structure of a nanotube [39–48], which, in turn, has an influence on its electron transport properties. A recent report has experimentally shown for the first time evidence of an electro-mechanical effect from strain in single-walled nanotubes, and also the first measurements of piezoresistive response in a self-contained nanotube-based nano-electro-mechanical structure [48].

We postulate that the binding of cancer cells simultaneously to multiple antibodies anchored to a nanotube creates a surface strain that changes the band gap and the conductivity of the nanotube. The putative increase in band gap due to cell binding effect would result in a decrease in conductivity. In general tensile stress increase the band gap and compressive stress decrease the band gap of carbon nanotube [39–48]. It has been seen in recent reports that for all semiconducting nanotubes, application of a torsional strain <0.1% leads to an increase in band gap, thereby decreasing the conductivity of the device [48]. Whether the strains are tensile, compressive or torsional, the increase or decrease in band gap is associated with the competing effects between elongation or contraction of the carbon bonds in the hexagon.

Our results support this hypothesis, implying that the strain originates on the surface of the nanotube due to biomolecular interactions and therefore can be used as a 'fingerprint' for molecular recognition. Specific interactions create much higher free energy change than non-specific interaction and therefore the strain and the associated band gap changes should be higher for specific antibody–receptor binding. For example, a free energy release of -150 kcal for antigen–antibody binding on the surface of the nanotube could generate a 1D stress of about 62.7 GJ m^{-1} over the length of the nanotube $\sim$10 μm. Since the nanotube is not free to move, the strain energy can only be transferred effectively along the length of the nanotube. This has been seen in the past where stress transfer is most effective for aligned nanotube systems along their length [49]. Assuming the Young's modulus of the nanotube to be 1.2 Tpa [50], the strain observed along the length of the nanotube could be as high as 5.225% for this free energy change, far higher than strains reported for band gap changes. This is due to the large free energy released during binding over a small area of the device. However, it should also be pointed out that not all the free energy released is used as work to strain the nanotube. Part of it could be dissipated to the surrounding liquids as heat. Future studies using AFM could reveal the actual stress on the surface of the nanotube upon antibody binding to their corresponding receptors.

Now pointing our attention to band gap, for example, the band gap of (16, 0) SWCNT with 2% tensile strain is about 30% larger than that of the unstrained (16, 0) SWCNT, which results in reduced source to drain current [51]. Using this argument it can be estimated that for a 5.2% tensile strain on the nanotube, the resulting conductivity should decrease by about 50–60% due to an increase in band gap, which is what our measured results indicate. On the other hand torsional strains are only known to be associated with band gap increases [51]. Under torsion, there are mainly three carbon bonds that are responsible for band gap changes. The bonds perpendicular to the axial direction, remains constant, while the other two bonds one elongates and other contracts. It has been reported that for a torsional angle of 36°, the compression strain of the bond that shortens in length is 0.7% whereas the tensile strain of bond that elongates is 3%. The bonds perpendicular to the length of the nanotube only deforms by 0.07% [52]. Therefore the band gap changes associated even with torsion will depend on the bonds that deform the most and in this case the bonds that elongates. In other words even a large torsion results in a tensile loading of the nanotube and therefore increases the band gap as seen in past reports [48]. It is therefore estimated that the strains seen in our

devices should either be tensile or torsional depending on the arrangement of the antibodies and the nanotube chirality, both resulting in reduced conductivity. Past work in tuning band gap using strains have shown ∼100 meV per 1% stretch in carbon nanotube [53]. Using this argument, one can estimate a band gap increase ∼0.5 eV for our device which is a high estimate. Future work in this area using atomic force microscopy can reveal the nature of strain itself on the nanotube surface.

Specific antibodies create much higher change in free energy upon binding to their antigens compared to non-specific antibodies [1, 36, 37]. This has also shown to be true for ligand–receptor interaction using atomic force microscope [54]. Therefore the stress on the surface of the nanotube and the accompanying change in the electron transport properties must be higher for specific pairs compared to non-specific pairs as our results indicate (60% reduction in conductivity for specific pairs compared to ∼10% reduction for non-specific pairs). The origin of stress and the change in conductivity can therefore be used as a 'fingerprint' for sensing various different types of biomolecules without labeling.

The high sensitivity and specificity of the nano-electro-mechanical device that is described here combined with the ability to create single or small bundle nanotube devices can decrease the cost of these devices. While nanowire devices have been used in the past to sense cancer proteins in blood [15], they are purely electrical in nature and there is no strain associated with conformational change of proteins on nanowire surface. All the nanowire devices show an increase in conductivity on specific binding [15]. Network of nanotube devices also show an increase in conductivity associated with conformational change of proteins on their surface [17]. The electrical conductivity change due to mechanical stress generated by biomolecules that we present here is unique and has much higher specificity originating from the stress due to biomolecular interactions that are often specific in nature. Only hollow structures such as a single nanotube can respond to such small strains and change their conductivity as has been seen in theory and AFM experiments in the literature [39–48].

There are many important differences in the devices described here. The present devices can directly sense cancer cells in blood, without the need for much further modification. Second, the design of our devices with small electrode spacing and a single nanotube for probing allows us to sense single cancer cells. While we flow 100 000 cells, the device becomes independent of the number of cells around as soon as a single cancer cell reaches the spacing between the electrodes. In other words, once the cell arrives at the electrode, the device performs like an on–off quantum bit. The isolation of the entire device from other areas using a polymer except the spacing makes the number of cells that are present in the surrounding areas irrelevant. In other words, the cells that bind to the antibodies on the surface of the nanotube between the electrodes can only result in changes in the electrical transfer characteristics. Further, the device is different from past nanotube devices that have been used to monitor free protein interactions. Past nanotube devices used networks of nanotubes [16, 17]. Only single or small bundle (1–10) nanotubes can change their band gap readily due to the presence of strain that is measured electronically in line with existing literature [39–48]. The hollow nature of the nanotube and since most of the atoms in single wall nanotubes are surface atoms, small strains can be accompanied by change in C–C bond that can change the band gap and conductivity.

Approximating a roughly spherical shape for a circulating malignant cancer cell, the volume of the cancer cell can be estimated to be 6×10^{-16} l. However, it should be noted that the entire volume of the cell does not interact with the antibodies. Only 1/10th of the cell (cell diameter 10 μm, spacing between electrodes 1 μm) interacts with the device. It is estimated that there are as many as one million IGF1R receptors on a rapidly proliferating MCF7 breast cancer cell [25]. Since we estimated about 10–12 antibodies functionalized on the surface of each nanotube, the estimated volume sensitivity of our device is estimated to be $\sim10^{-13}$–10^{-14} l of proteins, which is more sensitive than any known device today.

This level of sensitivity is clinically relevant. Such an array could in principle be used as a hand-held device to sense directly circulating tumor cells or proteins or DNA in blood in one step without the need for additional reagents or processing. Second, the use of arrays can be used to conduct multiple bioassays in a single run, thereby increasing the information content and decreasing time for a single test. Such devices could also be used in locations where access to health care facilities is minimal. The label-free option makes it particularly attractive for drug discovery, which requires one to detect specific binding between small molecules with proteins. One disadvantage of this device may is that the single cancer cell has to reach the spacing between the electrodes. However, that can be overcome very easily by using a micro-fluidic channel and allowing the blood to flow through the channel.

5. Conclusions

There are many innovations in the work that is presented here: first, the single nanotube electronic device that we report here for cancer cell detection is fabricated by airbrushing [26, 27], rather than by e-beam lithography [28, 29], which is time consuming and expensive. The nanotubes are aligned between lithographically patterned electrodes using the torque generated by the flow of air, prior to subsequent lithography and metalization steps, to ensure reliable and stable contacts. Such a protocol ensures both high yields, low cost, and acceptable performance.

Second, the cancer cell that is detected here, ∼10 μm in diameter, is 10–15 times larger than the spacing between the nanotube contact electrodes. While we use live cells in our experiments, it is only the proteins that are precisely sensed that makes this technology viable for sensing DNA, proteins as well as cells in blood. The electrodes are completely isolated from the cell by an insulating coating. Therefore, when a cell comes in contact with the device, only the antibodies on the surface of the nanotube can contact the surface of the cell, as all the other areas of the device are isolated. The change in conductivity can therefore only arise from the interaction of cell surface proteins with antibodies that are functionalized on the nanotube surface. Thus, each SWCNT-mAb junction functions as an on–off quantum bit.

Third, the device is unique due to the use of a single/small bundle of nanotubes that can respond to changes in stress on its surface and change its conductivity. Networks of nanotubes tend to be more conductive than single nanotube devices, thereby masking the actual biological events and producing low signal to noise ratio.

This new technology for live cancer cell detection is label-free, displays single cell sensitivity, high selectivity, high reproducibility, easy fabrication, and low cost compared to nanoscale top-down manufacturing. We postulate that the change in free energy associated with multiple simultaneous cell–antibody–nanotube interactions generates a stress on the surface of the nanotube that decreases its conductivity.

In the future, we will design and build arrays of SWCNT-mAb devices targeting multiple cell surface proteins simultaneously to identify particular kinds of cancer cells. Parallel, multicomponent detection will reveal the presence of 1, 2, 3, or more cancer cells in a volume of blood that covers multiple junctions.

Acknowledgments

The authors wish to acknowledge the funding for this research provided by DAMD W81XWH-06-1-0668, NSF CAREER award ECS 0546328, and NIH INBRE 2 P20RR016472-06 subproject to Balaji Panchapakesan, and by DOE/BER ER63055 and NIH/NCI CO_2 7175 to E W.

References

[1] Wu G, Datar R H, Hansen K M, Thundat T, Cote R J and Majumdar A 2001 Bioassay of prostate specific antigen using microcantilevers *Nat. Biotechnol.* **19** 856–60

[2] Whelan J P, Kusterbeck A W, Wemhoff G A, Bredehorst R and Ligler F S 1993 Continuous flow immunosensor for detection of explosives *Anal. Chem.* **65** 3561–5

[3] Devine P J *et al* 1995 A fiberoptic cocaine biosensor *Anal. Biochem.* **227** 216–24

[4] Zhu H *et al* 2000 Analysis of yeast protein kinases using protein chips *Nat. Genet.* **26** 283–9

[5] Davies H, Lomas L and Austen B 1999 Profiling of amyloid beta peptide variants using SELDI protein chip arrays *Biotechniques* **27** 1258–61

[6] Heegaard N H and Kennedy R T 1999 Identification, quantitation and characterization of biomolecules by capillary electrophoretic analysis of binding interactions *Electrophoresis* **20** 3122–33

[7] Mullett W, Lai E P and Yeung J M 1998 Immunoassay of fumonisins by a surface plasmon resonance biosensor *Anal. Biochem.* **258** 161–7

[8] Rubio I, Buckle P, Trutnau H and Wetzker R 1997 Real-time assay of the interaction of a GST fusion protein with a protein ligate using resonant mirror technique *Biotechniques* **22** 269–71

[9] Nicholson S, Gallop J L, Law P, Thomas H and George A J 1999 Monitoring antibody responses to cancer vaccination with a resonant mirror biosensor *Lancet* **353** 808

[10] Ostroff R M *et al* 1998 Fixed polarizer ellipsometry for simple and sensitive detection of thin films generated by specific molecular interactions: applications in immunoassays and DNA sequence detection *Clin. Chem.* **44** 2031–5

[11] Piehler J *et al* 1997 Label-free monitoring of DNA–ligand interactions *Anal. Biochem.* **249** 94–102

[12] Jones V W, Kenseth J R, Porter M D, Mosher C L and Henderson E 1998 Microminiaturized immunoassays using atomic force microscopy and compositionally patterned antigen arrays *Anal. Chem.* **70** 1233–41

[13] Blonder R *et al* 1996 Application of redox enzymes for probing the antigen–antibody association at monolayer interfaces: development of amperometric immunosensor electrodes *Anal. Chem.* **68** 3151–7

[14] Dahint R, Bender F and Morhard F 1999 Operation of acoustic plate mode immunosensors in complex biological media *Anal. Chem.* **71** 3150–6

[15] Zheng G, Patolsky F, Cui Y, Wang W U and Leiber C M 2005 Multiplexed electrical detection of cancer surface markers with nanowire sensor arrays *Nat. Biotechnol.* **23** 1294–301

[16] Chen R J, Zhang Y, Wang D and Dai H 2001 Noncovalent sidewall functionalization of single-walled carbon nanotubes for protein immobilization *J. Am. Chem. Soc.* **123** 3838–9

[17] Star A, Tu E, Niemann J, Gabriel J-C P, Steve Joiner C and Valcke C 2006 Label free electrical detection of DNA hybridization using carbon nanotube network field effect transistors *Proc. Natl Acad. Sci.* **103** 921–6

[18] de Bono J S *et al* 2007 Potential applications for circulating tumor cells expressing the insulin-like growth factor-I receptor *Clin. Cancer Res.* **13** 3611–6

[19] Nagrath S *et al* 2007 Isolation of rare circulating tumour cells in cancer patients by microchip technology *Nature* **450** 1235–9

[20] Miyazono F, Takao S, Natsugoe S, Uchikura K, Kijima F, Aridome K, Shinchi H and Aikou T 1999 Molecular detection of circulating cancer cells during surgery in patients with biliary-pancreatic cancer *Am. J. Surg.* **177** 475–9

[21] Surmacz E 2000 Function of the IGF-I receptor in breast cancer *J. Mammary Gland Biol. Neoplasia* **5** 95–105

[22] Surmacz E 2003 Growth factor receptors as therapeutic targets: strategies to inhibit the insulin-like growth receptor *Oncogene* **22** 6589–97

[23] Sachdev D and Yee D 2001 The IGF system and breast cancer *Endocr. Relat. Cancer* **8** 197–209

[24] Pollak M 1998 IGF-I physiology and breast cancer *Recent Results Cancer Res.* **152** 63–70

[25] Tian X, Aruva M R, Qin W, Zhu W, Duffy K T, Sauter E R, Thakur M L and Wickstrom E 2004 External imaging of CCND1 cancer gene activity in experimental human breast cancer xenografts with ^{99m}Tc–peptide–peptide nucleic acid-peptide chimeras *J. Nucl. Med.* **45** 2070–82

[26] Shao N, Lu S, Wickstrom E and Panchapakesan B 2007 Integrated molecular targeting of IGF1R and Her2 surface receptors and destruction of breast cancer cells using single wall carbon nanotubes *Nanotechnology* **18** 315101

[27] Panchapakesan B, Cesarone G, Lu S, Teker K and Wickstrom E 2005 Conductivity sensing of breast cancer cells by carbon nanotubes coated with monoclonal antibodies against IGF1 receptor *Nanobiotechnology* **1** 353–60

[28] Hedberg J, Dong L and Jiao J 2005 Air flow technique for large scale dispersion and alignment of carbon nanotubes on various substrates *Appl. Phys. Lett.* **86** 143111

[29] Lay M D, Novak J P and Snow E S 2004 Simple route to large-scale ordered arrays of liquid-deposited carbon nanotubes *Nano Lett.* **4** 603–6

[30] Teker K, Wickstrom E and Panchapakesan B 2006 Biomolecular tuning of electron transport properties of carbon nanotubes via antibody functionalization *IEEE Sensors* **6** 1422–8

[31] Martel R, Schmidt T, Shea H R, Hertel T and Avouris Ph 1998 Single-and multi-wall carbon nanotube field-effect transistors *Appl. Phys. Lett.* **73** 2447–9

[32] Bachtold A, Hadley P, Nakanishi T and Dekker C 2001 Logic circuits with carbon nanotube transistors *Science* **294** 1317–20
[33] Bradley K, Briman M, Star A and Gruner G 2004 Charge transfer from adsorbed proteins *Nano Lett.* **4** 253–6
[34] Heller I, Jannessens A M, Mannik J, Minot E D, Lemay S G and Dekker C 2008 Identifying the mechanism of sensing using carbon nanotube transistors *Nano Lett.* **8** 591–5
[35] Abramson H A and Moyer L S 1936 Electrical charge of mammalian red blood cells *J. Gen. Physiol.* **19** 601–7
[36] Fritz J, Baller M K, Lang H P, Rothuizen H, Vettiger P, Meyer E, Güntherodt H-J, Gerber Ch and Gimzewski J K 2000 Translating biomolecular recognition into nanomechanics *Science* **288** 316–8
[37] Wu G *et al* 2001 Origin of nanomechanical cantilever motion generated from biomolecular interactions *Proc. Natl Acad. Sci. USA* **98** 1560–4
[38] Janin J and Chothia C 1990 The structure of protein–protein recognition sites *J. Biol. Chem.* **265** 16027–30
[39] Heyd R, Charlier A and McRae E 1997 Uniaxial-stress effects on the electronic properties of carbon nanotubes *Phys. Rev.* B **55** 6820–4
[40] Kane C L and Mele E J 1997 Size, shape, and low energy electronic structure of carbon nanotubes *Phys. Rev. Lett.* **78** 1932–5
[41] Rochefort A, Avouris P, Lesage F and Salahub D R 1999 Electrical and mechanical properties of distorted carbon nanotubes *Phys. Rev.* B **60** 13824–30
[42] Yang L, Anantram M P, Han J and Lu J P 1999 Band-gap change of carbon nanotubes: effect of small uniaxial and torsional strain *Phys. Rev.* B **60** 13874–8
[43] Yang L and Han J 2000 Electronic structure of deformed carbon nanotubes *Phys. Rev. Lett.* **85** 154–7
[44] Maiti A, Svizhenko A and Anantram M P 2002 Electronic transport through carbon nanotubes: effects of structural deformation and tube chirality *Phys. Rev. Lett.* **88** 126805
[45] Ding J W *et al* 2003 Curvature and strain effects on electronic properties of single-wall carbon nanotubes *J. Phys.: Condens. Matter* **15** L439–45
[46] Guo G Y, Liu L, Chu K C, Jayanthi C S and Wu S Y 2005 Electromechanical responses of singlewalled carbon nanotubes: interplay between the strain-induced energy-gap opening and the pinning of the Fermi level *J. Appl. Phys.* **98** 044311
[47] Tombler T W *et al* 2000 Reversible electromechanical characteristics of carbon nanotubes under local probe manipulation *Nature* **405** 769–72
[48] Hall A R *et al* 2007 Electromechanical response of single wall carbon nanotubes to torsional strain in a self-contained device *Nat. Nanotechnol.* **2** 412–6
[49] Lu S, Ahir S V, Terentjev E M and Panchapakesan B 2007 Alignment dependent mechanical responses of carbon nanotubes to light *Appl. Phys. Lett.* **91** (10) 103106
[50] Lu J P 1997 Elastic properties of carbon nanotubes and nanoropes *Phys. Rev. Lett.* **79** 1297–300
[51] Yoon Y and Guo J 2007 Analysis of strain effects in ballistic carbon nanotube FETs *IEEE Trans. Electron Devices* **54** 1280–8
[52] Yu W, Xi W X and Xiangui N 2004 Atomistic simulation of torsion deformation of carbon nanotubes *Modelling Simul. Mater. Sci. Eng.* **12** 1099–107
[53] Minot E D, Yaish Y, Park J Y and McEuen P L 2003 Tuning carbon nanotube bandgaps with strain *Phys. Rev. Lett.* **90** 156401
[54] Moy V T, Florin E-L and Gaub H E 1994 Intermolecular forces between ligands and receptors *Science* **266** 257–9